Environmental mapping and screening of the offshore wind potential in Denmark

Impacts on waves

Danish Energy Agency

Date: 9. May 2025

Rev.no.	Date	Description	Prepared by	Verified by	Approved by
02	20250414	Rev 2	TEB/FRGR	KLBU/RHO	LRM
03	20250509	Rev 3	TEB	RHO	LRM

Contents

NOMENCLATURE

Abbreviation	Description
DEM	Digital Elevation Model
DTM	Digital Terrain Model
WGS84	World Geodetic System 1984
UTM	Universal Transverse Mercator
VD	Vertical Datum
MSL	Mean Sea Level
NCCS	Norwegian Center for Climate Services
BHS	German Federal Maritime and Hydrographic Agency
MEA	Mean Absolute Error
MWD	Mean Wave Direction
H_s	Measured Significant Wave Height
H_{m0}	Modelled Significant Wave Height
T_p	Peak Wave Period
RMSE	Root Mean Squared Error
SMHI	Swedish Meteorological and Hydrological Institute
SI	Scatter Index

1. Preface

Background for the report and relation to other activities

This report contributes to the project "*Environmental mapping and screening of the offshore wind potential in Denmark"* initiated in 2022 by the Danish Energy Agency. The project aims to support the long-term planning of offshore wind farms by providing a comprehensive overview of the combined offshore wind potential in Denmark. It is funded under the Finance Act 2022 through the programme "Investeringer i et fortsat grønnere Danmark" (Investing in the continuing greening of Denmark). The project is carried out by NIRAS, Aarhus University (Department of Ecoscience) and DTU Wind.

The overall project consists of four tasks defined by the Danish Energy Agency (https://ens.dk/energikilder/planlaegning-af-fremtidens-havvindmoelleparker):

1. Sensitivity mapping of nature, environmental, wind and hydrodynamic conditions.
2. Technical fine-screening and assessment of the overall offshore wind potential based on the sensitivity mapping and relevant technical parameters".
3. Assessment of potential cumulative effects from large-scale offshore wind development in Denmark and neighbouring countries.
4. Assessment of barriers and potentials in relation to coexistence.

This report addresses one component of Task 1: sensitivity mapping. Specifically, it provides an overview of areas within Danish offshore regions that are likely to be particularly vulnerable to offshore wind farm development regarding waves based on wind provided by DTU Wind considering the wind without wind farms and with the wind farms in the year 2021 and 2030.

The project has relied predominantly on historical data, with minimal new data collection. As a result, the sensitivity mapping is largely dependent on the availability and accessibility of pre-existing data across specific subject areas. From the outset, significant effort was made to incorporate all relevant data to comprehensively address the task requirements. However, certain existing datasets could not be accessed. Section 4 specifies the data sources used in the sensitivity mapping for waves and outlines additional existing data. It is important to recognize that sensitivity mapping serves as a dynamic tool, which can be updated as new data becomes available.

The project management teams at both AU and NIRAS have contributed to the description of the background for the report and the relation to other activities in the preface. The report and the work contained within are solely the responsibility of the authors.

2. Summary

The purpose of this report is to illustrate the spatial impact of wind farms on the wave climate[1] in the North Sea, Kattegat, and Baltic Sea and to map the sensitivity.

The report will cover, in order:

- The collection of background data to generate inputs for the Significant Wave model (SW).
- The collection of data for validation of the SW model, including:
    - Wave data such as significant wave height (**H_s**, average height of the highest one-third of waves in a given sea state) and peak period (**T_p**, time interval between wave crests in the most energetic part of the wave spectrum).
- A description of the methodology applied in the study, from model setup to result processing.
- Calibration performed on the Baseline scenario – the scenario without wind turbines.
- Presentation of results, highlighting the effects of wind farms by comparing the Baseline scenario with the Current (2021) and Future (2030) wind farm scenarios.

The wind farm settings for the Current and Future scenario are illustrated in Figure 2.1, which highlights the distinction between the offshore wind turbines currently in place and those scheduled for installation over the next six years.

The MIKE 21 Spectral Wave Model (SW) was used to simulate wave climates under different wind farm configurations, considering factors like wind, the individual wind turbine substructure, bathymetry, and wave interactions.

The model was calibrated using wave buoy recordings from 2019, ensuring an accurate representation of wave dynamics and propagation.

The study determined that Current scenario have a minimal impact on wave conditions[2], while Future scenario may significantly reduce wave heights, especially in Danish waters and in the area between the Netherlands and England (coincident with a high density of wind turbines, up to 12 MW/km^2) (Hahmann, et al., 2025).

Changes in wave conditions due to the presence of wind farms affect the longshore sediment transport capacity, with the most substantial impacts expected in eastern Denmark. The influence on longshore sediment transport capacity is more significant than that on wave conditions. For the Current scenario, the variation is primarily within +2% to -5%, whereas for Future scenario, this range could expand to approximately +2% to -20%.

[1] Refers to the average wave conditions in a particular area over an extended period, typically months or years. It encompasses the typical wave heights, periods, and directions that are expected in that region, providing insight into the general "climate" of the waves in that area.

[2] Refers to the general condition of the waves in a specific area at a particular moment in time. It encompasses factors such as wave height, wave period (the time between waves), wave direction, and wavelength. In essence, it describes the wave characteristics in that area at that specific point in time.

Although the findings indicate that offshore wind farms may affect coastal processes, the current analysis utilizing longshore transport capacity does not yield sufficient data to draw definitive conclusions about long-term shoreline evolution or morphological changes associated with actual longshore sediment transport.

The results conclude that while current wind farms have a limited impact on the waves, future large-scale developments will have more pronounced effects on wave climate and sediment transport capacity.

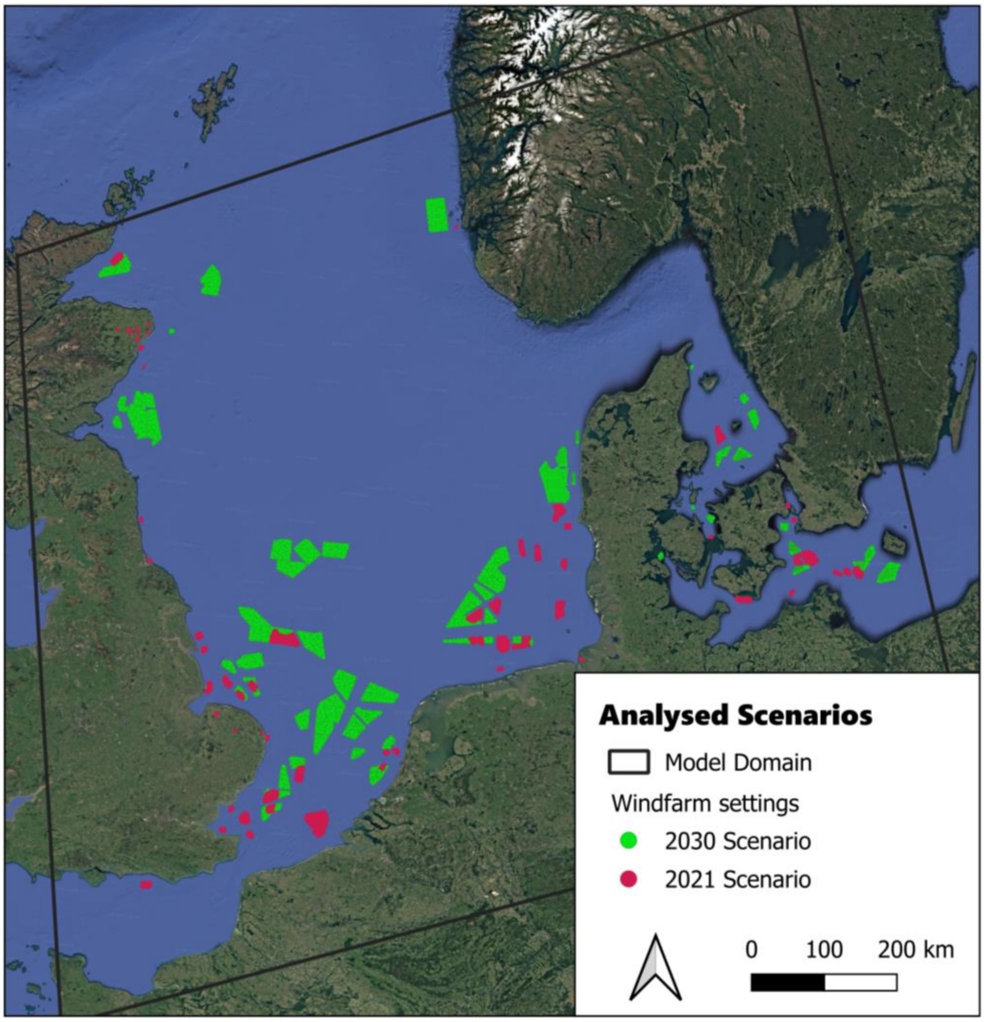

Figure 2.1: Overview of the location of the Current scenario (pink) and of the Future scenario (green) in the North Sea, Kattegat, and the Baltic Sea.

3. Introduction

Large-scale offshore wind farms have been documented to affect hydrodynamics both within and beyond the wind farms, extending over many kilometres. These effects include a reduction in wind resource efficiency behind large wind farms due to the wake effect, along with localized impacts from turbine foundations.

Water transport, current conditions, waves, resuspension, sediment transport, salinity, and temperature may also be affected, causing changes in mixing and stratification patterns. These hydrodynamic alterations have the potential to impact environmental conditions and exacerbate oxygen depletion in areas within and around wind farms (Ute Daewel, Naveed Akhtar, Nils Christiansen & Corinna Schrum, 2022).

3.1. Scope of Work

The aim of this report is to produce a sensitivity map showing how the presence of wind farms in the North Sea, Kattegat and Baltic Sea affects the wave climate and longshore sediment transport capacity. For this purpose, a spectral wave model was used to simulate the following three cases:

1) **Baseline scenario:** a scenario without any wind farm installed based on the wind in 2019.
2) **Current scenario, 2021:** current situation including existing Danish offshore wind turbines utilising the wind in 2019.
3) **Future scenario, 2030:** scenario following the future large-scale offshore wind development in Danish Sea areas: the North Sea, Kattegat, Belts, and the Baltic Sea utilising the wind in 2019.

The scenarios are executed based on DTU WIND's calculations and using the 2D MIKE Spectral Wave model by DHI. For further description of the method see section 5.

4. Background data

The upcoming sections provide the background information utilized for numerical modelling. This chapter encompasses descriptions of metocean and meteorological conditions, such as wave observations and bathymetric data and wind data.

4.1. Coordinate System

Unless stated otherwise, the Vertical Datum (*VD*) throughout the report is Mean Sea Level (*MSL*), while the geographic coordinate system is WGS84 EPSG 7416 ETRS89 UTM32N.

4.2. Bathymetry

One of the main inputs of the model is the Digital Terrain Model (***DTM***). A DTM is a digital representation of the terrain or ground surface of a specific area or location. It is a three-dimensional model that provides information about the elevation, slope, and other topographic features of the terrain.

DTMs are created using Digital Elevation Models (***DEM***s), which are datasets that provide information about the elevation of the ground surface.

The Digital Terrain Model (DTM) used for the SW model originates from the combination of two different sources of data: the European Marine Observation and Data Network 2023 (EMODnet, 2023), reported in Figure 4.1, and the digital nautical charts obtained from the application MIKE C-Map from DHI, shown in Figure 4.2.

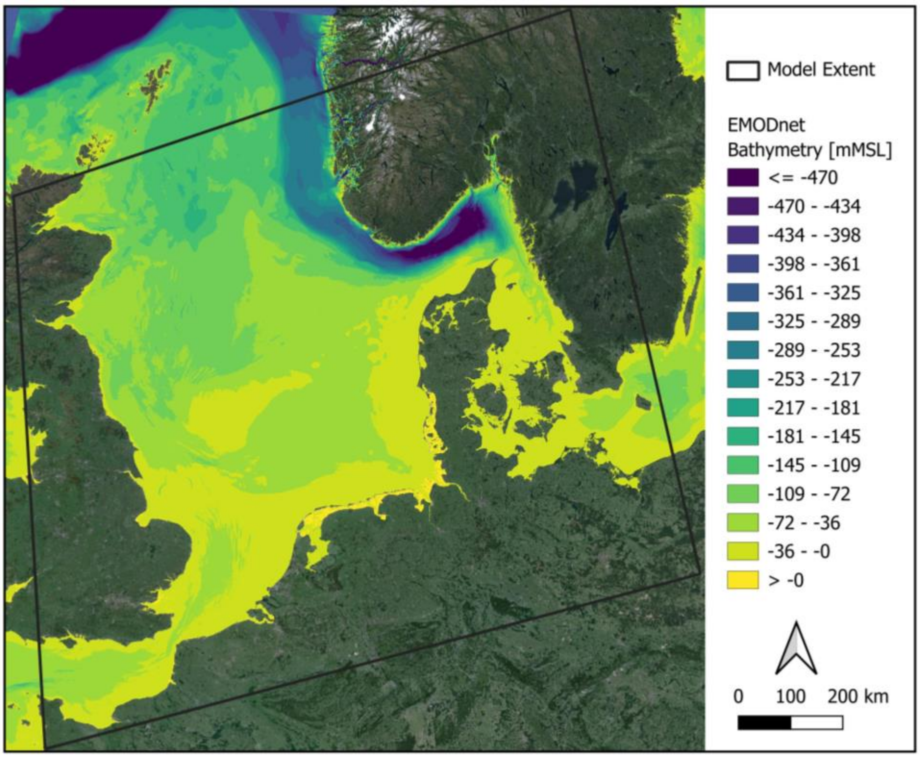

Figure 4.1: Extent of the model area (black box) with EMODnet bathymetry used for the interpolation of the mesh for the spectral wave model.

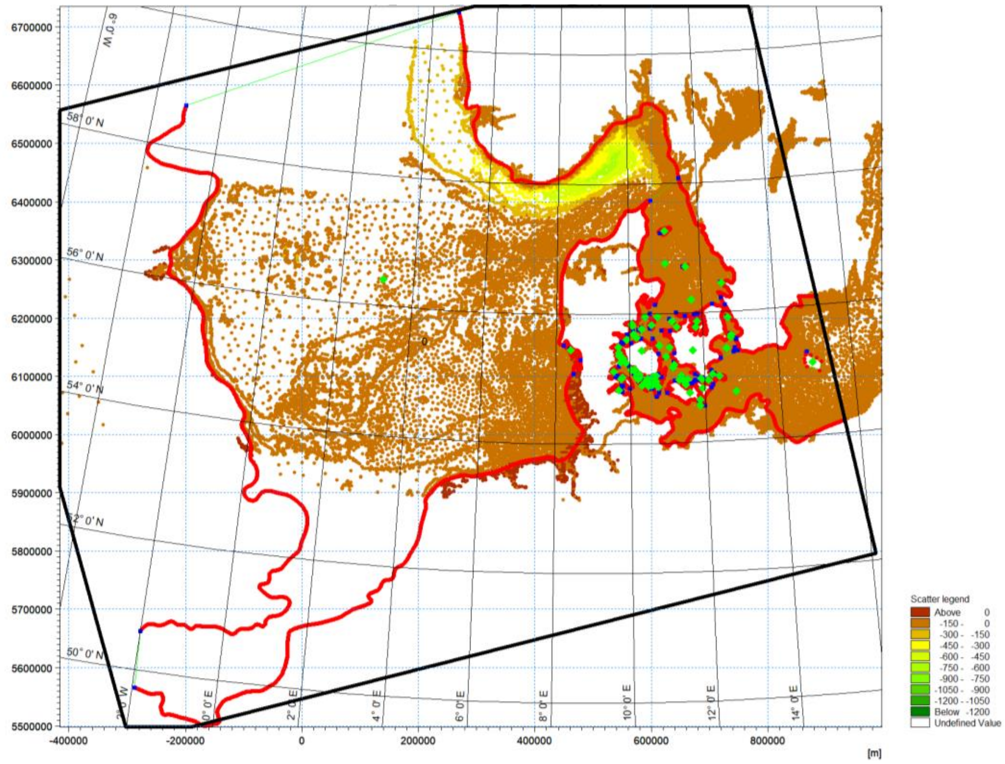

Figure 4.2: MIKE C-Map scatter data of water depths for the North Sea and Baltic Sea used for the interpolation of the mesh for the sw modelling.

4.3. Wind Forcing

Wind and pressure used as forcings for the simulations have been developed by DTU Wind and are described in detail in (Hahmann, et al., 2025).

4.4. Wave Observations

To validate/calibrate the model, wave buoy recordings related to the simulated period (January-December 2019) are key for an accurate description of the physical processes. Three sources of data provided wave measurements within the area of study:

- The Copernicus Marine In Situ TAC: The In Situ TAC component of the Copernicus Marine Service ensures consistent and reliable access to a range of in situ data for the purpose of service production and validation.
- The Swedish Meteorological and Hydrological Institute database (SMHI).
- The Norwegian Center for Climate Services (NCCS).
- The German Federal Maritime and Hydrographic Agency (BSH), which provides in the "Report on the oceanographic conditions at site O-1.3" (German Federal Maritime and Hydrographic Agency (BSH), 2021) a description of the marine monitoring instrument that record at a location close to the Arkona Basin.

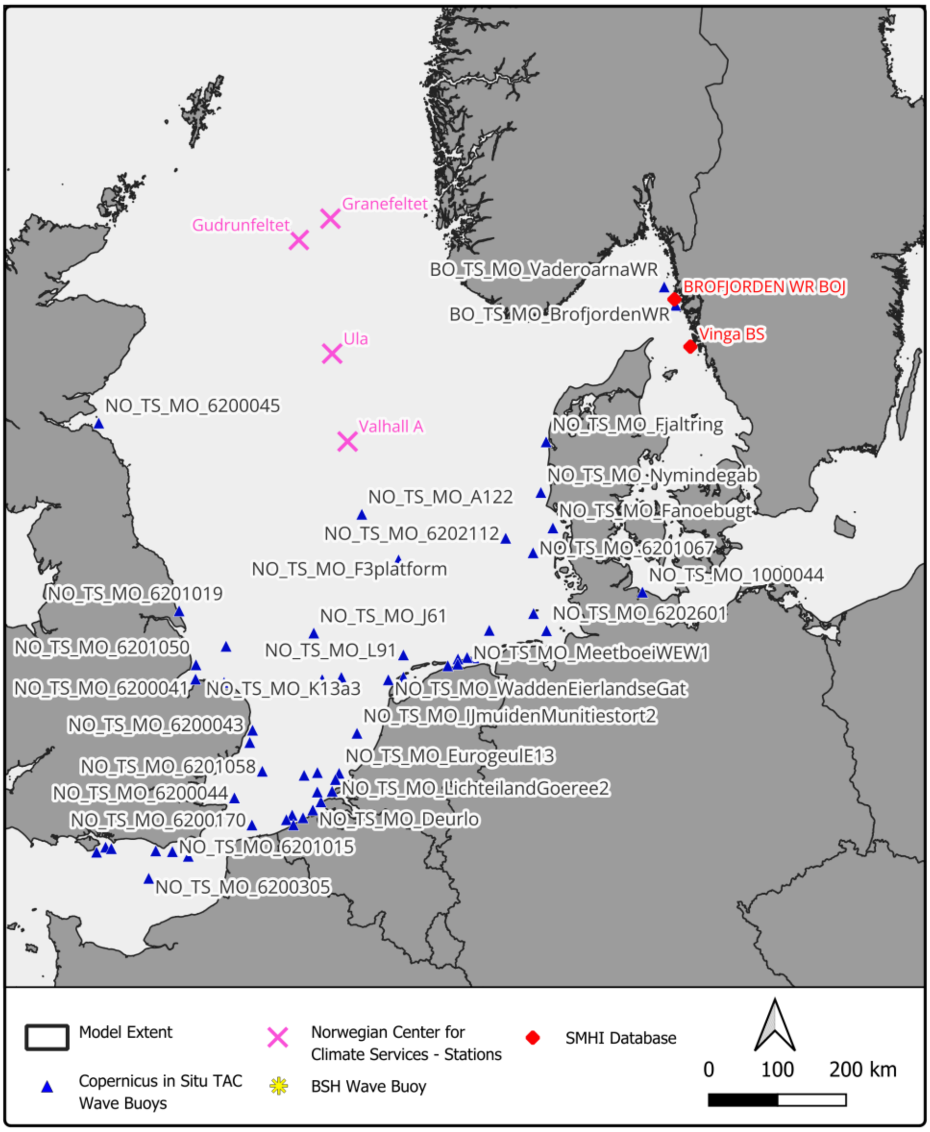

Figure 4.3: Location of the retrieved wave measurements.

The retrieved observed wave data are characterized by significant wave height (H_s), peak period (T_p), and mean wave direction (MWD). However, although all stations recorded H_s, only a few provided information on period and direction.

The collected measurement data underwent a comprehensive quality check to determine which stations provided reliable time series of wave parameters and which could only be used to evaluate the general patterns of the simulated wave data. A description of each recovered measurement station, i.e. location, time zone, and coverage (%) is reported Appendix A.

Three representative stations for each side were selected to be following reported, while the time-series of H_s and T_p for the other stations are placed in Appendix B.

The stations selected for comparison and reported in the main body of this report are listed in Table 4.1 and shown in Figure 4.1.

Table 4.1: Stations selected for calibration of the SW model.

Station ID	Longitude [deg]	Latitude [deg]	Time	Coverage (%)
NO_TS_MO_F3platform	4.727	54.853	UTM0	95
NO_TS_MO_A122	3.816	55.417	UTM0	85
Valhall A	3.393	56.278	UTM1	100

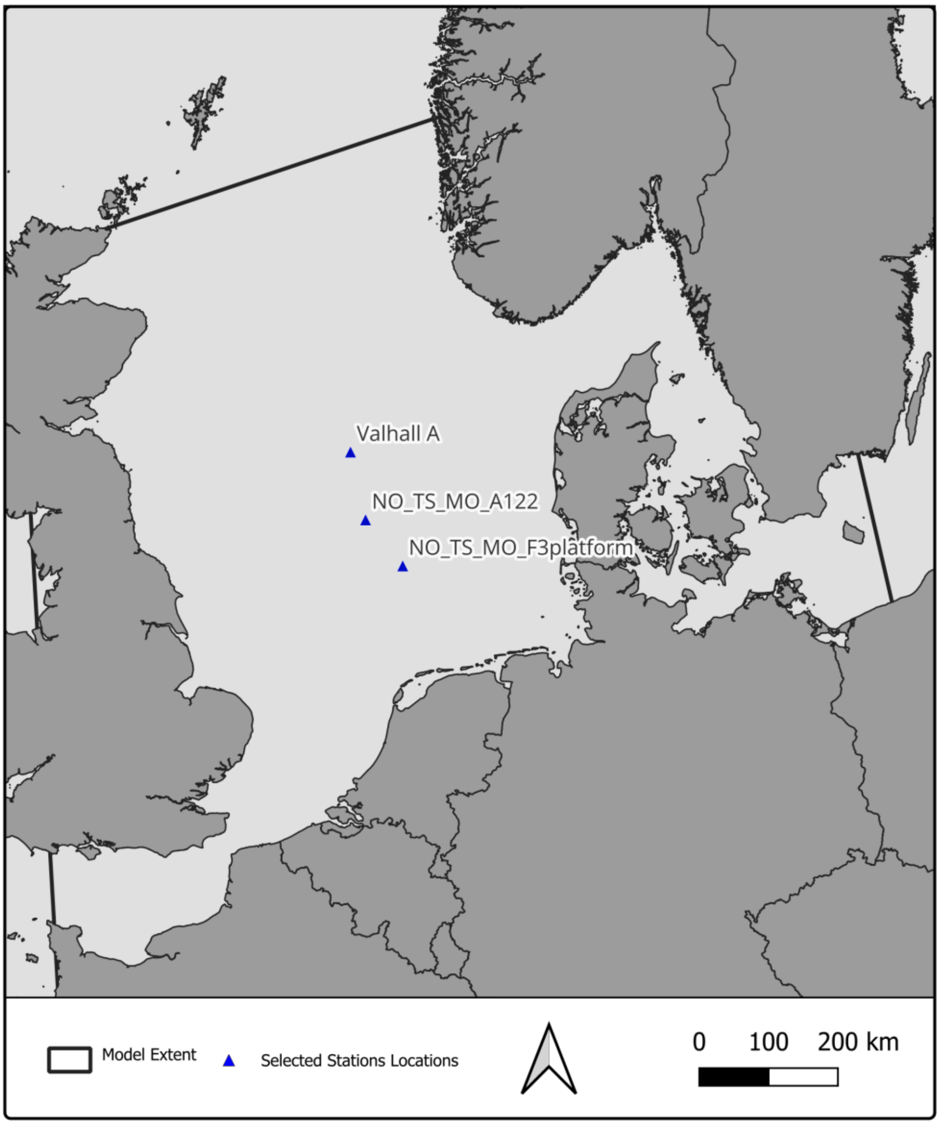

Figure 4.1: Location of the stations selected for calibration of the SW model.

The time series of significant wave height and peak period (when available) for each of the selected stations is reported in Figure 4.2 to Figure 4.4

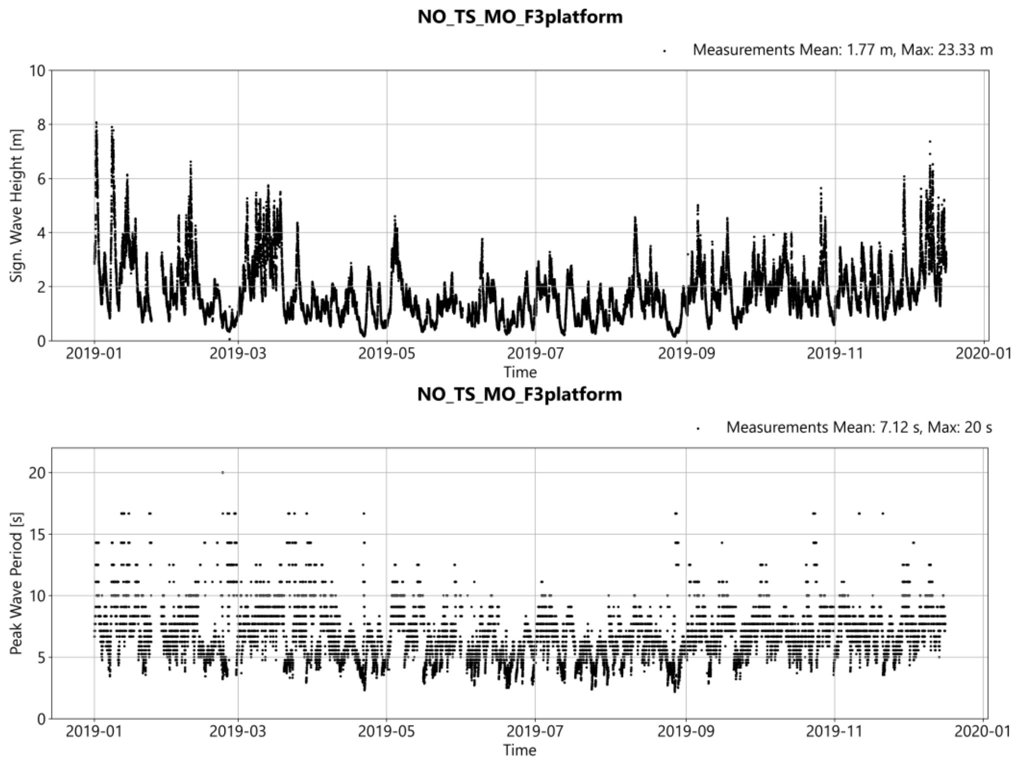

*Figure 4.2: Significant wave height (top) and peak period (bottom) recorded at the station **NO_TS_MO_F3platform.***

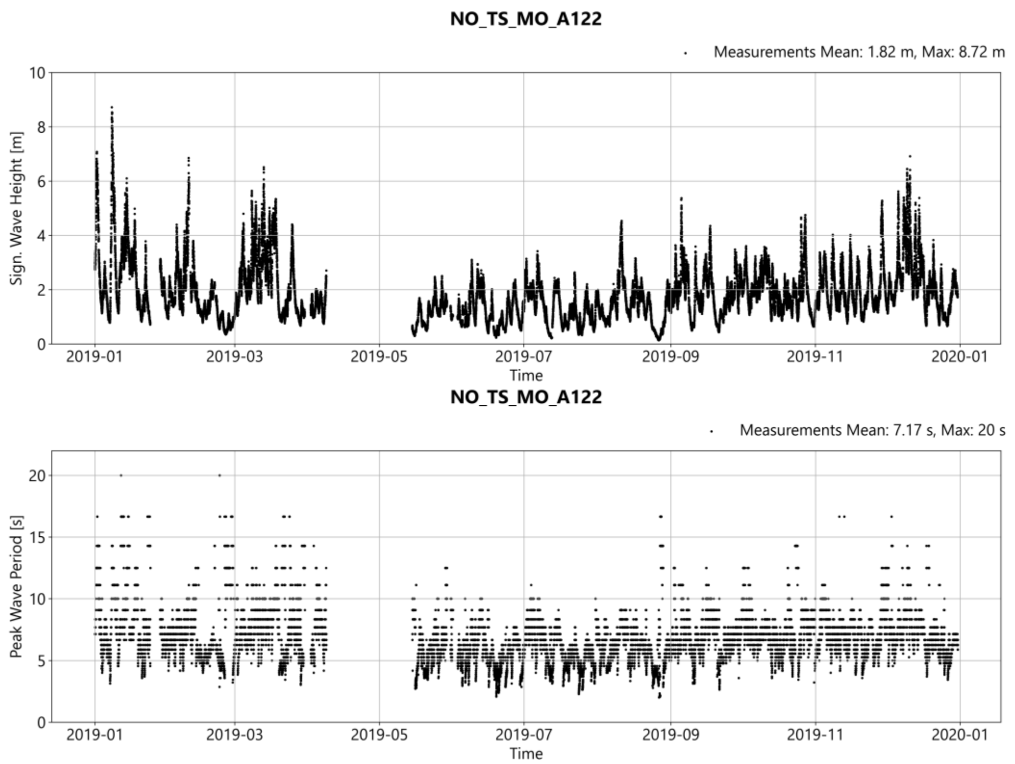

*Figure 4.3: Significant wave height (top) and peak period (bottom) recorded at the station **NO_TS_MO_A122.***

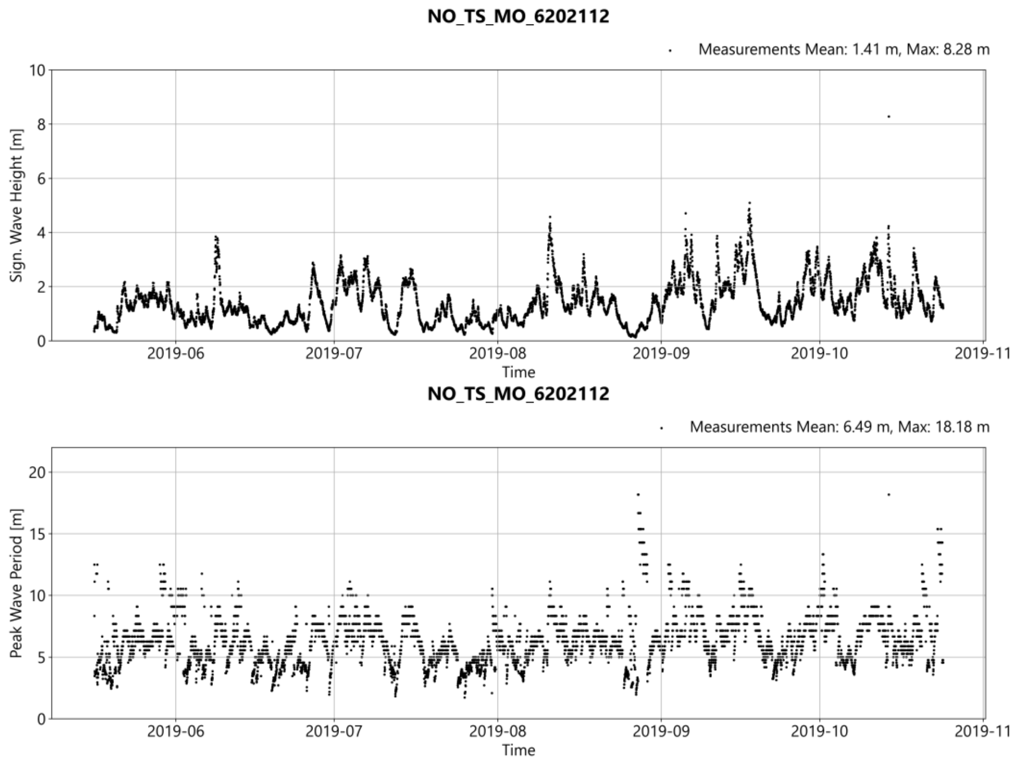

*Figure 4.4: Significant wave height (top) and peak period (bottom) recorded at the station **NO_TS_MO_6202112**.*

The comparison between the wave parameters recorded at three selected stations and the modelling results are presented and discussed in Section 6.3.

It is important to highlight that in the case of the retrieved Arkona Basin station, there is a 30-minute interval between recordings and the time steps never correspond to the simulated time step. The data was interpolated in order to be compared to the spectral wave model results.

5. Methodology

A spectral wave model was used to simulate the wave climate in Danish waters to assess the impact of the current and future offshore wind farms. For each scenario, a distinct wind forcing file was applied, all reflecting wind conditions from 2019, but accounting for varying configurations of wind farms; Current scenario (2021 wind farms) and Future scenario (2030 wind farms), within the study area.

Prior to assessing potential impacts, the base model is calibrated using the collected wave measurements mentioned above, see Section 4.4.

Taking into account the effects of different wind farm configurations on the wave climate, the sediment transport capacity was estimated using the CERC formulation (Leo Vanrjin, Delft, Netherlands) for the Current and Future scenarios and then compared to the rate observed in the Baseline scenario.

5.1. Spectral Wave model

MIKE 21 Spectral Wave Model (SW) is a computer-based simulation tool used for analyzing and predicting wave characteristics in coastal and offshore environments.

The MIKE 21 Spectral Wave Model utilizes spectral wave theory to simulate the transformation and propagation of ocean waves. It takes into account various factors such as wind, currents, bathymetry (seafloor topography), and wave interactions to accurately predict wave height, direction, period, and other wave parameters.

The SW module is capable of modelling the growth, decay, and transformation of wind-sea and swell waves in coastal and offshore areas. Its engine includes the following physical processes:

- Wave growth by wind,
- Non-linear wave-wave interaction,
- Wave-current interaction,
- Dissipation of energy due to white capping,
- Dissipation of energy due to bottom friction,
- Dissipation of energy due to depth-induced wave breaking,
- Refraction and shoaling due to variation in water depth,
- Effect of time-varying water depth and currents,
- Effect of ice coverage,
- Diffraction,
- Reflection and
- Influence of structures such as Wave/Tidal Energy Converters (WEC/TEC)

The main computational features in MIKE 21SW are:

- Source functions based on state-of-the-art 3rd generation formulations,
- Fully spectral and directionally decoupled parametric formulations,
- In-stationary and quasi-stationary solutions,
- Optimal degree of flexibility in describing the bathymetry and the ambient flow conditions using depth-adaptive and boundary fitted unstructured mesh,
- Coupling with hydrodynamic flow module for modelling wave-current interaction and time-varying water depth,
- Flooding and drying in connection with time-varying water levels,
- Extensive range of model output parameters (e.g. wind-sea, swell, air-sea interaction parameters, radiation stresses, wave spectra, etc.) and

- Parallelization using Open MP and MPI techniques.

The model uses a flexible mesh based on unstructured triangular or quadrangular elements and applies a finite volume numerical solution technique. The version 2024 of MIKE 21 Spectral Wave SW was used in the present study. Further details are provided in (DHI A/S, 2021).

5.2. Kamphius formulation

The Kamphuis formulation is an empirical model used to estimate longshore sediment transport, incorporating a range of coastal parameters to improve accuracy over simpler methods. Unlike more basic formulations, the Kamphuis equation accounts for variables like wave height, wave period, sediment grain size, beach slope, and wave angle. This makes it particularly useful in applications where site-specific characteristics significantly influence sediment movement along the shore.

The Kamphius 1991 formula, see Equation 1 reported in (Leo Vanrjin, Delft, Netherlands), is an improvement of the CERC formulation for the longshore sediment transport.

$$Q_l = 2.33(T_p)^{1.5}(tan\beta)^{0.75}(d_{50})^{-0.25}(H_{s,br})^2[sin(2\theta_{br})]^{0.6}$$ *Equation 1*

Where:

- Q_l – Longshore sediment transport rate (m^3/year);
- T_p – Peak wave period (s);
- β – Beach slope (-);
- d_{50} – Median grain size of sediment (m);
- $H_{s,br}$ – Significant wave height at breaking (m);
- θ_{br}– Wave breaking angle relative to the shoreline (degN),

6. Model setup and calibration

This section introduces the core of the calculations in the present study: DHI's MIKE 21 SW module and the SW model built specifically for it.

6.1. Computational Grid

Figure 6.1 shows the computational mesh and boundaries of the SW model. The resolution of the SW model was selected as a balance between maintaining reasonable computational time.

The resolution progressively varies from the offshore area of the North Sea to the internal region between Sweden and Denmark, where the majority of the offshore wind farms are situated. Offshore and along the coasts of Great Britain and Germany, the resolution is 2 km², which decreases to 1 km² as it approaches the Baltic Sea.

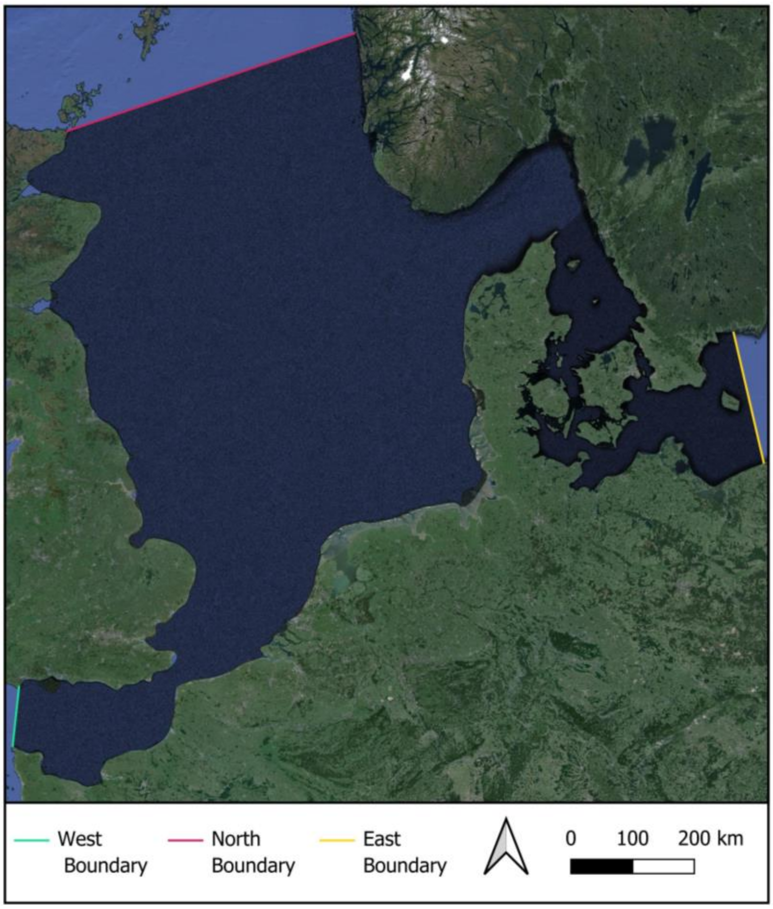

Figure 6.1: Computational mesh and boundaries defined for the spectral wave model of the North Sea, Kattegat, Belts and Baltic Sea.

6.2. Model Set-up

The model setup is summarized in Table 6.1. When not otherwise specified, the configuration of the SW model follows the default setup. Through a calibration process, the best fit between modelled data and measurements was obtained increasing the value of the air-water interaction parameters so that the energy dissipation within the domain decreased.

Table 6.1: Summary of the SW model settings.

Setting	Value
MIKE Version	MIKE 2024
Mesh resolution	6,417 km^2 (at the boundaries) to 23 km^2 (at the project area)
Simulation period	Jan 1st 2019 00:00 to Dec 31st 2019 23:00
Spectral Formulation	Fully Spectral formulation, Instationary Formulation
Energy Transfer	Included quadruplet-wave interaction
Growth parameter	1.3
Wave age tuning parameter	0.011
Background Charnock parameter	0.01
Atmospheric forcing	DTU generated Wind
Boundary Conditions	ERA5

6.3. Model Calibration

Time-series of the wave parameters H_{m0} (significant wave height as calculated by the spectral wave model), T_p and MWD were extracted at the wave buoys' locations and validated against the available measurements in order to calibrate the model and obtain an accurate description of the physical processes involved in the wave dynamics and propagation.

Three representative stations were selected to be reported in the following, while the comparison between the model results and the other stations is placed in Appendix C. The stations selected for comparison and reported in the present section are listed in Table 4.1.

The comparison between final model results and measurements is presented in terms of time-series, scatter plots and statistical coefficients such as:

- The **Correlation Coefficient**, which quantifies the strength of a linear relationship between two variables, with values from -1 to 1. A value of -1 indicates a perfect negative correlation, where one variable increases as the other decreases, while a value of 1 represents a perfect positive correlation, where both variables move in the same direction.
- The **Bias**, which refers to a systematic error that causes an estimator to deviate from the true population value. Bias occurs when the method of collecting, measuring, or interpreting data consistently skews results in a particular direction, leading to inaccurate or misleading conclusions.
- The **Mean Absolute Error** (MAE), representing the average magnitude of errors in a model's predictions, without considering their direction (positive or negative). It ranges from zero to infinity. A lower MAE indicates a model with more accurate predictions.
- The **Root Mean Square Error** (RMSE), that RMSE reflects the average magnitude of prediction error, with larger errors given more weight due to the squaring. The RMSE can range from zero to infinity, and a lower RMSE indicates more accurate predictions.
- The **Scatter Index** (SI) is a standard metric for wave model intercomparison and represents a normalized measure of error, can be presented as percentage. Lower values of SI correspond to a better match between observations and modelled values: according to "The impact of atmospheric model resolution on a coupled wind/wave forecast system" (Howard, et al., 2009), "in the context of significant wave height, reports of the scatter index (SI) in the literature range between from 0 to 20% (0.20) for hindcasts with sophisticated models and high quality wind fields".

The statistical coefficients are presented in Table 6.2, while the comparison of the time-series of measurements and modeled parameters is reported from Figure 6.1 to Figure 6.12 and Appendix C.

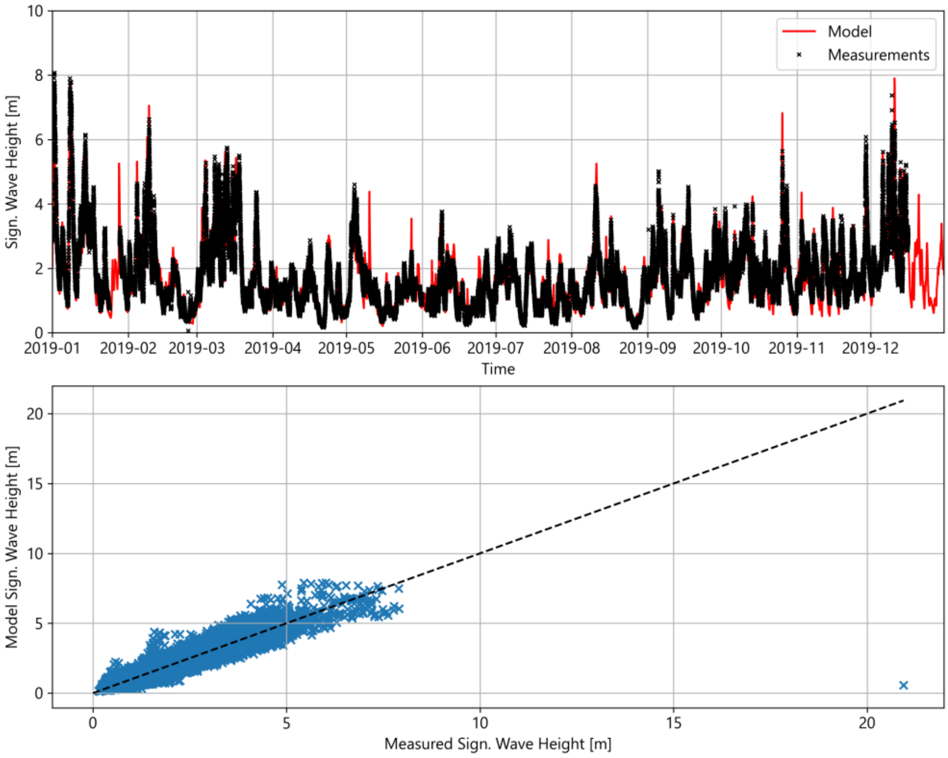

Figure 6.1: ***Station ID NO_TS_MO_F3platform*** *- Comparison model vs. measurements of yearly time series of the significant wave height.*

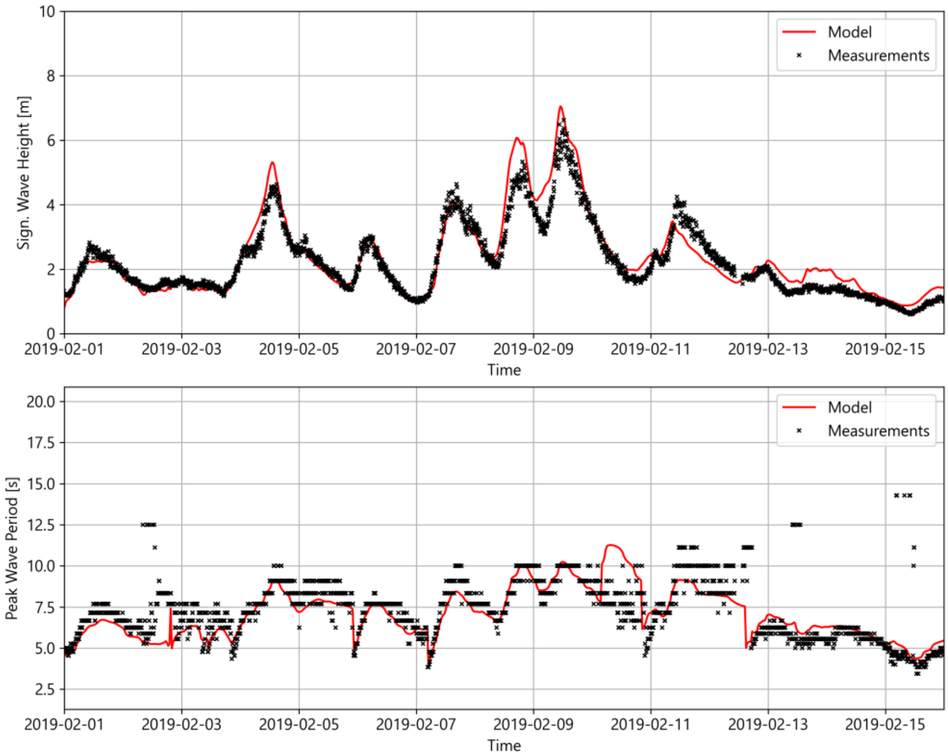

Figure 6.2: ***Station ID NO_TS_MO_F3platform*** *- Comparison model vs. measurements: time series of the significant wave height (top) and peak wave period (bottom). Period: 15-02-2019 to 01-03-2019.*

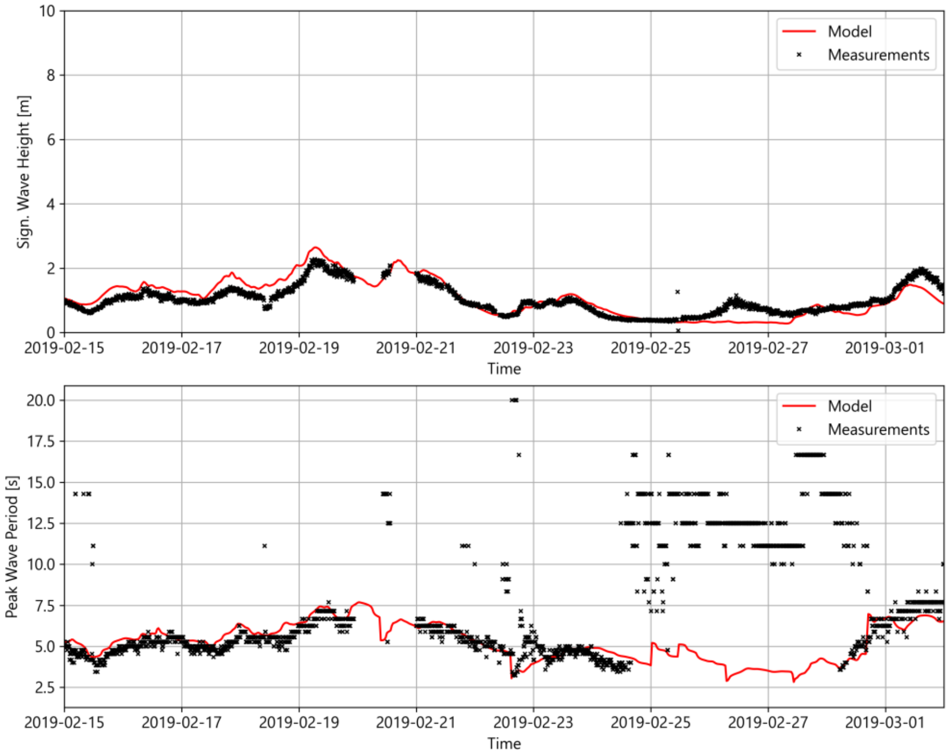

*Figure 6.3: **Station ID NO_TS_MO_F3platform** - Comparison model vs. measurements: time series of the significant wave height (top) and peak wave period (bottom). Period: 15-02-2019 to 01-03-2019.*

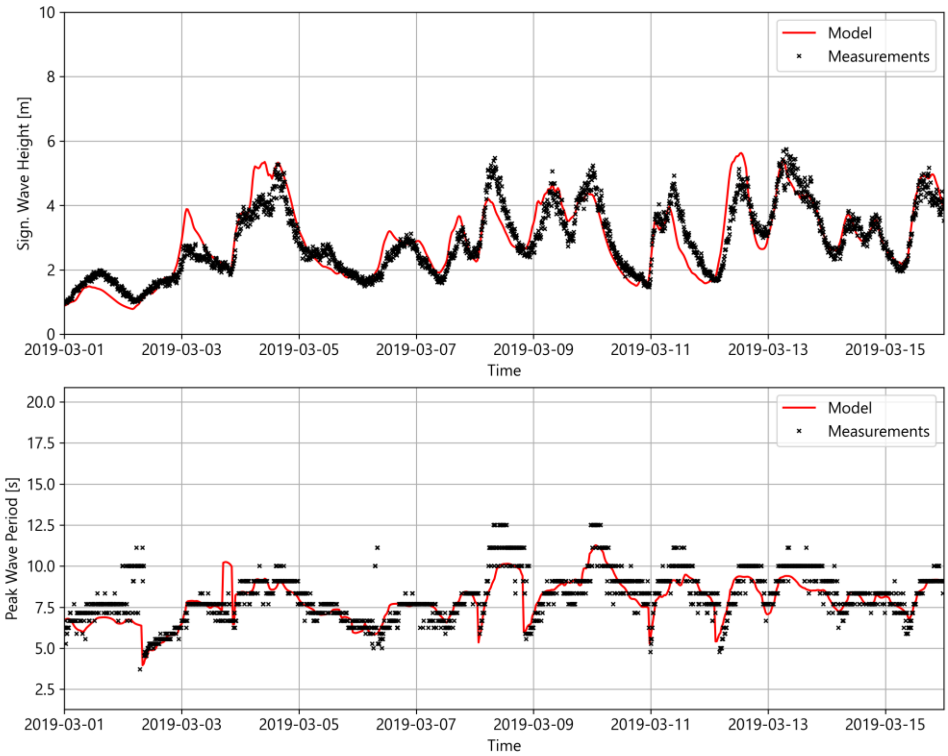

*Figure 6.4: **Station ID NO_TS_MO_F3platform** - Comparison model vs. measurements: time series of the significant wave height (top) and peak wave period (bottom). Period: 01-03-2019 to 15-03-2019.*

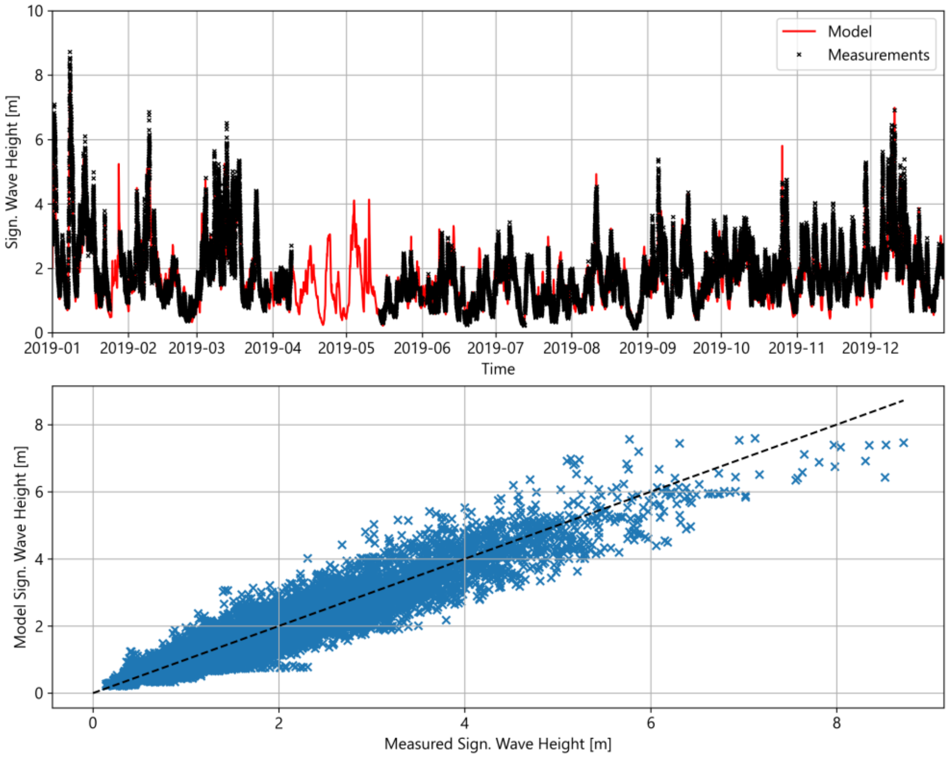

*Figure 6.5: **Station ID NO_TS_MO_A122** - Comparison model vs. measurements of yearly time series of the significant wave height.*

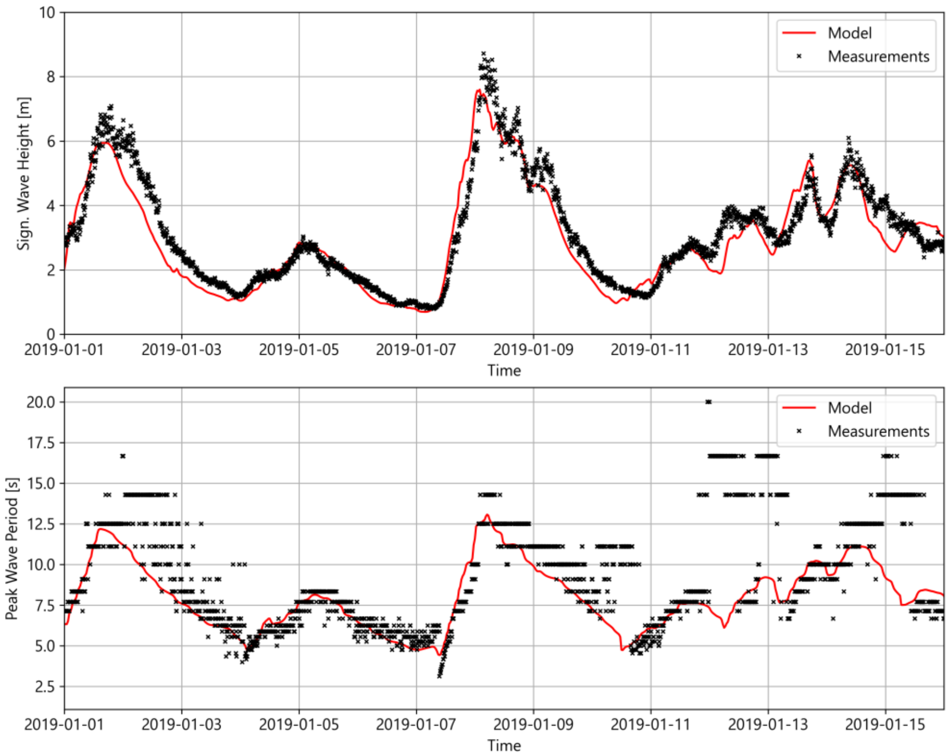

*Figure 6.6: **Station ID NO_TS_MO_A122** - Comparison model vs. measurements: time series of the significant wave height (top) and peak wave period (bottom). Period: 01-01-2019 to 15-01-2019.*

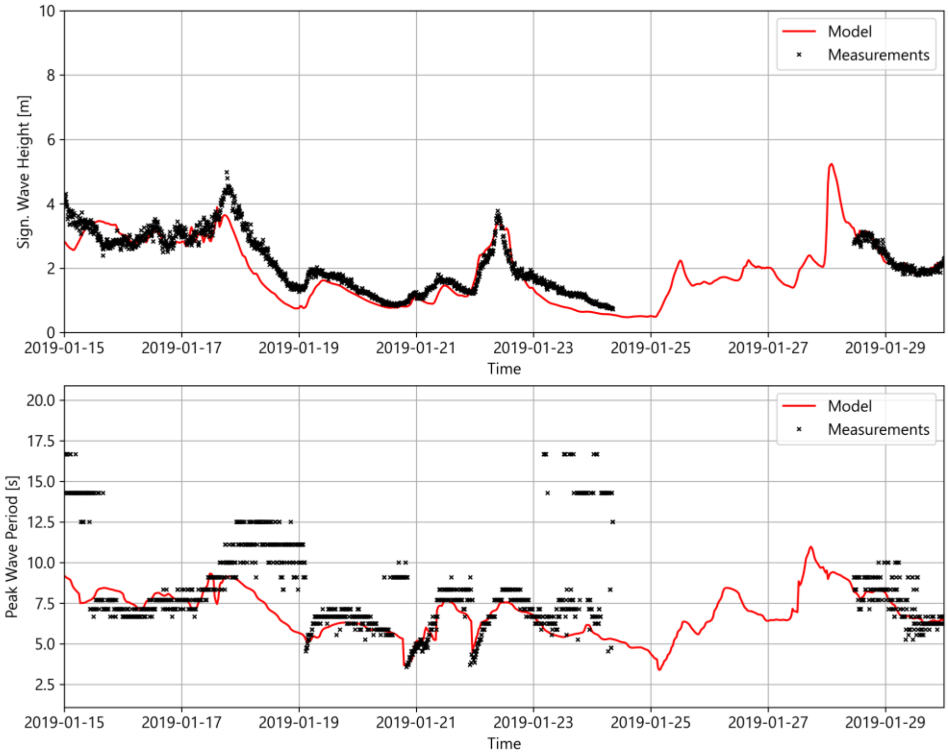

Figure 6.7: ***Station ID NO_TS_MO_A122*** *- Comparison model vs. measurements: time series of the significant wave height (top) and peak wave period (bottom). Period: 15-01-2019 to 01-02-2019.*

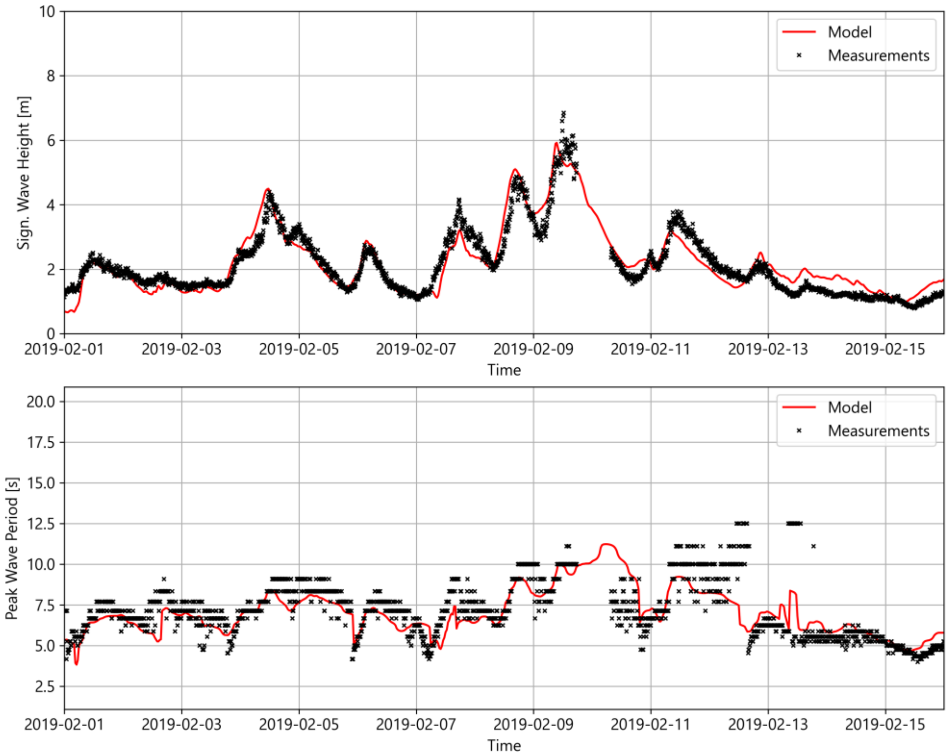

Figure 6.8: ***Station ID NO_TS_MO_A122*** *- Comparison model vs. measurements: time series of the significant wave height (top) and peak wave period (bottom). Period: 01-03-2019 to 15-03-2019*

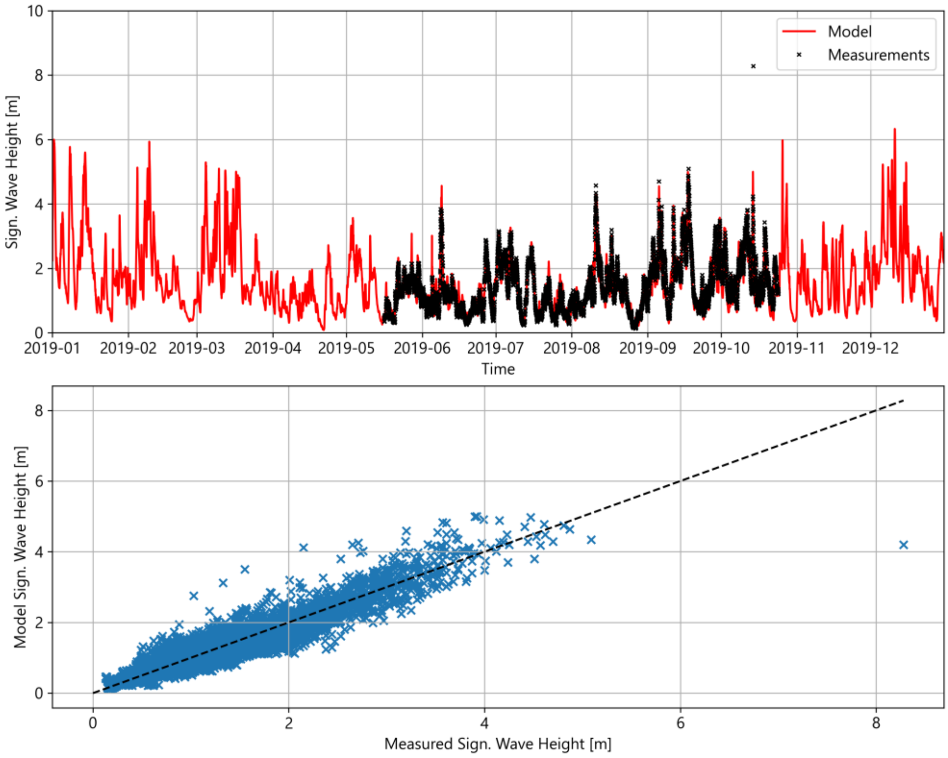

Figure 6.9: ***Station ID NO_TS_MO_6202112****- Comparison model vs. measurements of yearly time series of the significant wave height.*

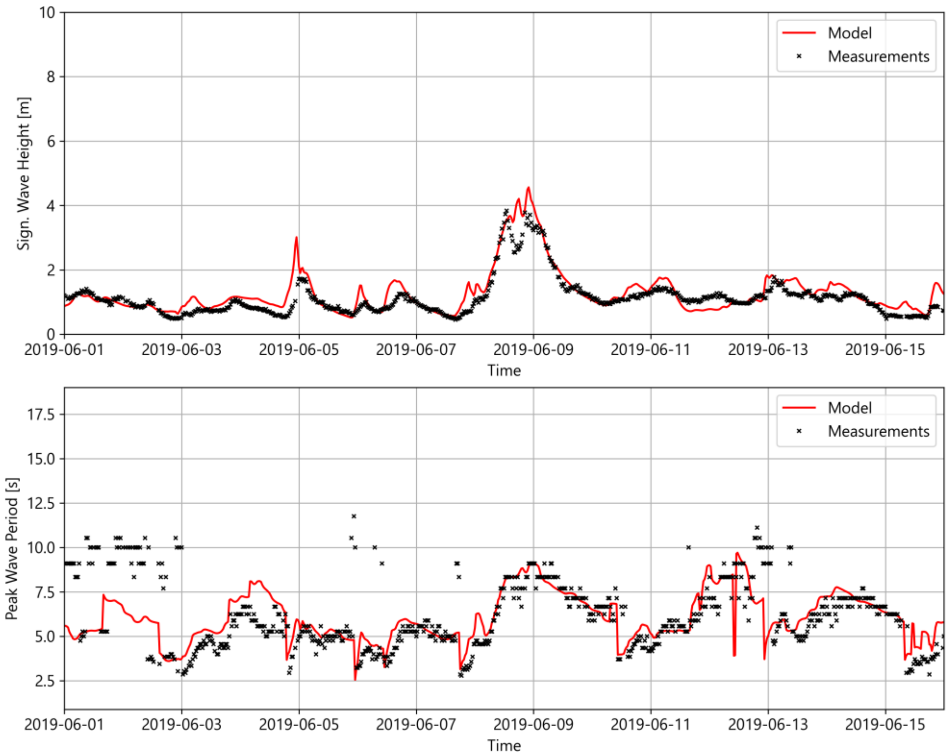

Figure 6.10: ***Station ID NO_TS_MO_6202112*** *- Comparison model vs. measurements: time series of the significant wave height (top) and peak wave period (bottom). Period: 01-06-2019 to 15-06-2019.*

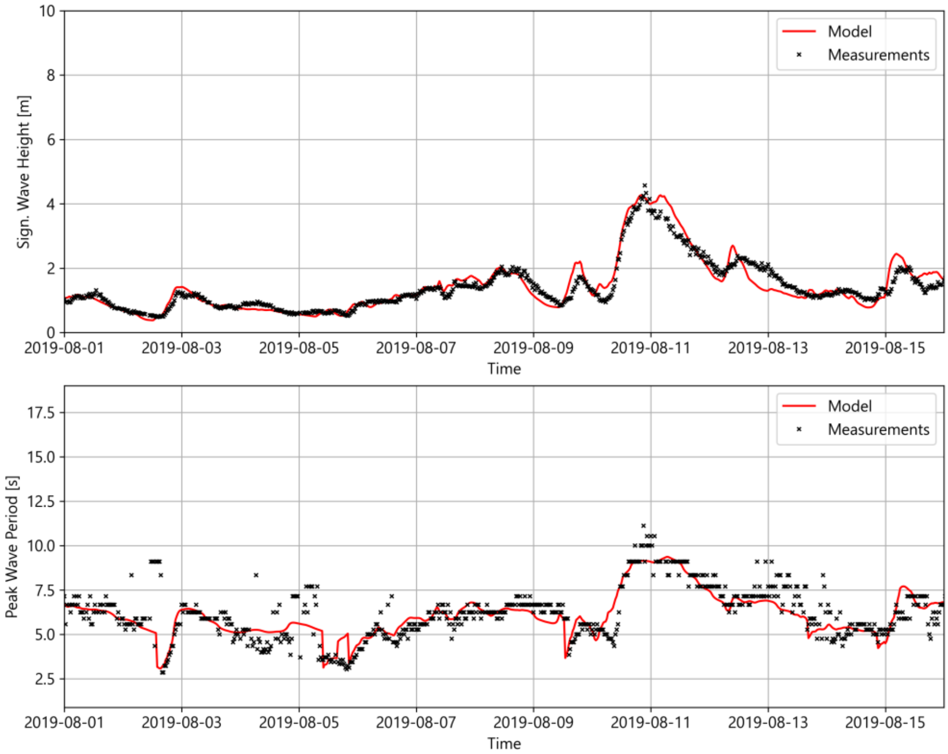

*Figure 6.11: **Station ID NO_TS_MO_6202112** - Comparison model vs. measurements: time series of the significant wave height (top) and peak wave period (bottom). Period: 01-08-2019 to 15-08-2019.*

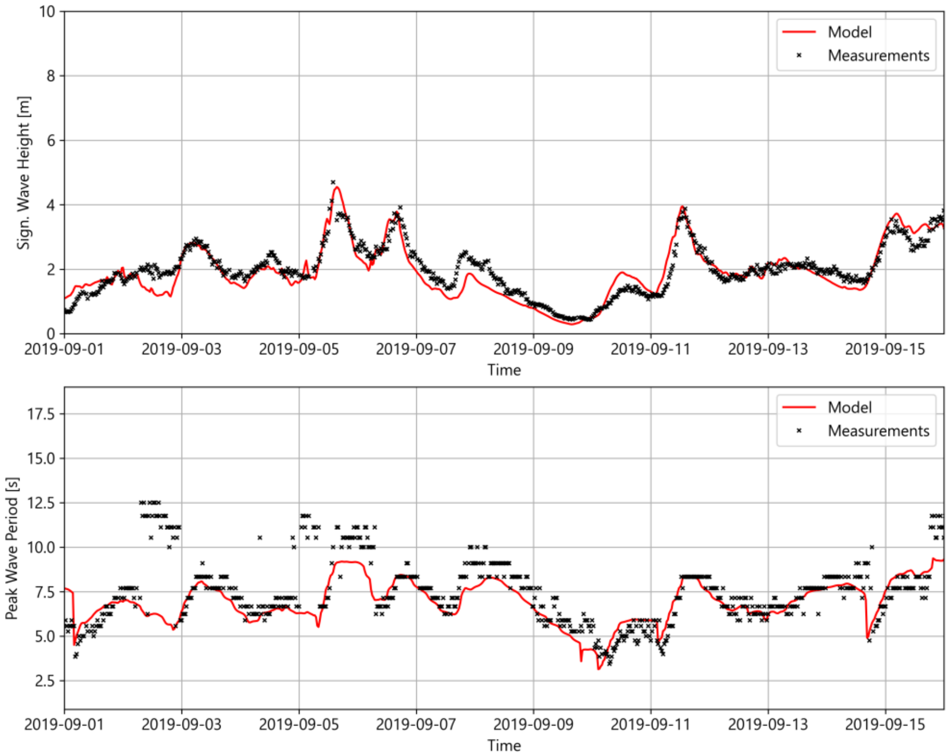

*Figure 6.12: **Station ID NO_TS_MO_6202112** - Comparison model vs. measurements: time series of the significant wave height (top) and peak wave period (bottom). Period: 01-09-2019 to 15-09-2019.*

Table 6.2: Correlation coefficient, Bias, MAE, RMSE and SI for the comparison between simulated and measured significant wave height at three selected locations (stations).

	Parameter: Sign. Wave Height				
Station ID	**Correlation Coefficient**	**Bias**	**MAE**	**RMSE**	**SI**
NO_TS_MO_F3platform	0.93	+0.11	0.22	0.33	0.23
NO_TS_MO_A122	0.94	-0.05	0.28	0.37	0.20
NO_TS_MO_6202112	0.93	+0.00	0.21	0.29	0.20

Despite the model's tendency to overestimate the peak values of significant wave height, the comparison figures indicate that the overall pattern of model results aligns well with the measurements. This is evidenced by a scatter index close to 0.2 and a correlation of 0.93 to 0.94, which is regarded as indicative of good agreement.

The comparison between the measurements recorded by station *Valhall A* and the modelled significant wave height show a shift in time that cannot be explained by differences in the time zone.

7. Results

The following sections present the results of the conducted modelling. Specifically, this chapter includes:

1. The wave parameters derived from the Baseline scenario (without wind farms) at three representative locations within the Danish EEZ (see Section 7.1),
2. The impact of wind farms on wave conditions under both the Current and Future scenarios (see Section 7.2),
3. The impact of wave height reduction, resulting from the presence and expansion of wind farms, on sediment transport capacity in both the Current and Future scenarios (see Section 7.3).

7.1. Baseline scenario

To enable the reader to comprehend the differences in wave climate within Danish waters, H_{m0} data was extracted from the Baseline scenario results—excluding the impact of wind farms—from three specific locations: one in the Baltic Sea, one in Kattegat, and one offshore Jutland in the North Sea west of Hvide Sande. The locations are shown in Figure 7.1 and the coordinates in Table 7.1.

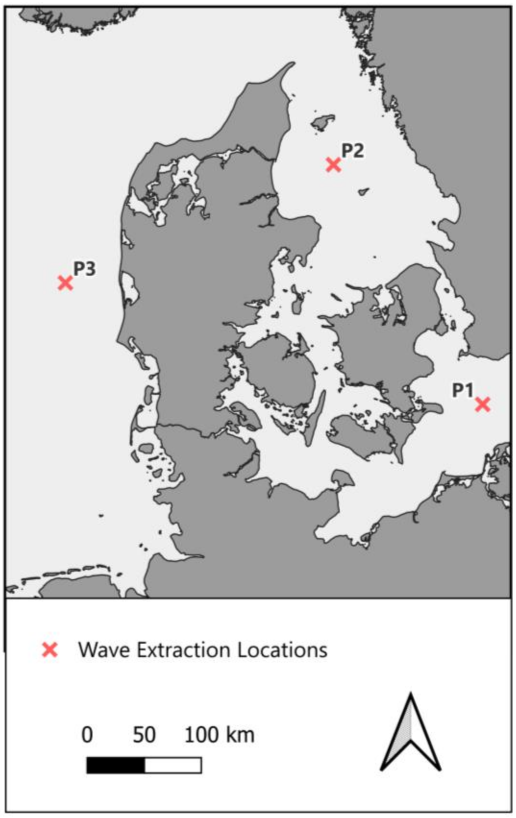

Figure 7.1: Locations of extraction of significant wave height and mean wave diretion.

Table 7.1: Description of the locations of extraction of wave conditions.

ID	X	Y	Area
P1	762483.01	6102118.35	Baltic Sea
P2	631675.33	6312239.29	Kattegat
P3	396695.01	6208658.55	North Sea

The annual wave roses for the three locations are shown in Figure 7.2, which highlights the following observations:

- For the Baltic Sea location (P1, first rose on the left), while the predominant wave direction in 2019 was from the Southwest, wave directions from west to northwest were equally significant in terms of magnitude,
- The Kattegat area data (P2, middle rose) reflects less directional dependency, likely due to its sheltered conditions and the fetch, in contrast to the more defined directional patterns observed at the other two sites,

  Like P1, the North Sea location (P3, off the Jutland coast) shows that the primary wave directions extend from north-northwest to south-southwest.

The annual wave roses for the three locations in Figure 7.1 are reported in Figure 7.2.

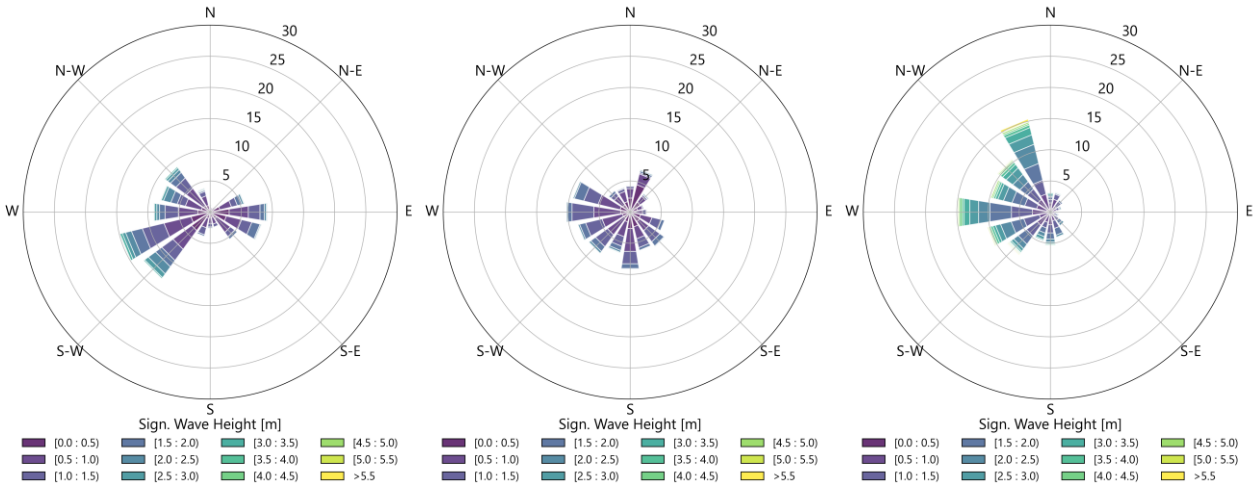

Figure 7.2: Annual wave rose for selected locations, from left to right, P1 (Baltic Sea), P2 (Kattegat) and P3 (North Sea).

7.2. Spatial Impact on Waves

The spatial impact of Current and Future scenario on wave climate is assessed by comparing the variations in significant wave heights (H_{m0}) between the two scenarios versus the Baseline scenario:

- Current scenario (i.e. year 2021) versus the Baseline scenario,
- Future scenario (i.e. year 2030) versus the Baseline scenario.

The difference is calculated for both the annual average and the monthly average, but only the annual results are included in the main body of this report. In addition to the overall results for the modelled area, a detailed analysis of the results within the Danish EEZ is presented.

To interpret the results, it is important to note that shades of blue indicate a decrease in H_{m0} from the Baseline scenario to the Current or Future scenario setting, whereas reddish colours represent an increase in H_{m0}.

Key results regarding the entire modelled area, annual spatial impact

- The results represent both the Current scenario and the Future scenario with changes in the annual significant wave height above 0.03 m mainly observed in the area surrounding the offshore wind farms,

- Current scenario: Referring to the entire modelled area, the installed wind farms generate little to no disturbance with respect to the significant wave height calculated in the absence of offshore wind farms. The modeled reduction in annual average H_{m0} ranges from 0.0 to -0.1 m,
- Future scenario: The additional wind farms increase the effect on the significant wave height compared to the scenario without wind farms (Baseline). In this case, the decrease in annual averaged H_{m0} ranges from 0.0 to more than -0.2 m, with the peak reached in the area between the Netherlands and England coinciding with the higher density of wind turbines.

Results are shown in Figure 7.3 and repeated in Figure 7.4 with marking of windfarm sites.

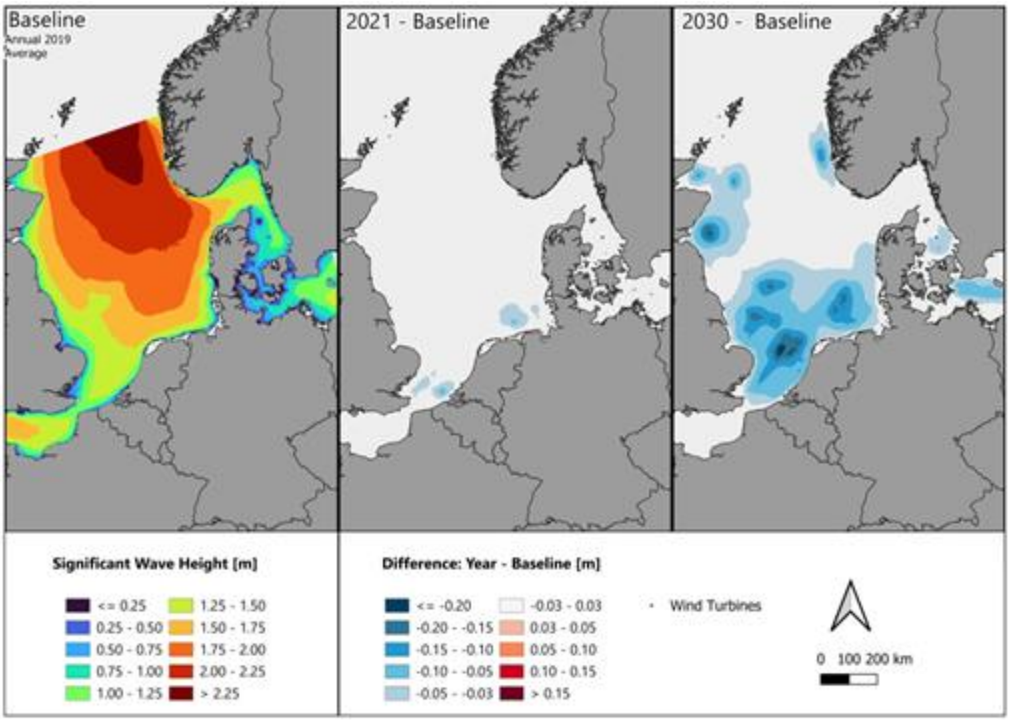

*Figure 7.3: **Whole model domain - Baseline and Baseline - Scenarios.** Left: annual average H_{m0} (m), Mid: Scenario 2021 minus Baseline, Right: Scenario 2030 minus Baseline*

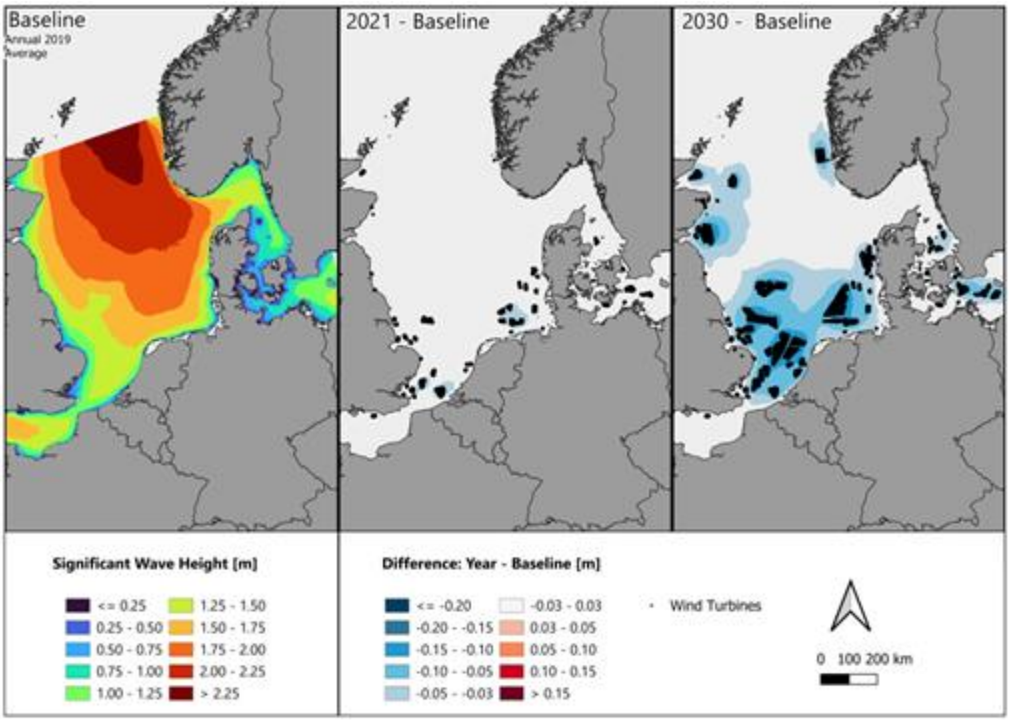

Figure 7.4: ***Whole model domain - Baseline and Baseline - Scenarios.*** *Left: annual average H_{m0} (m), Mid: Scenario 2021 minus Baseline, Right: Scenario 2030 minus Baseline. "Mid" and "Right" marked with the wind farms*

Key results regarding the Danish EEZ and Danish waters, annual spatial impact

- Current scenario: The per 2021 installed wind farms has a minimum effect on significant wave height, $H_{m0.}$ Reductions, in the order of 0.03 m, are only observed around Horns Rev and Kriegers Flak,
- Future scenario: The annual average of H_{m0} is clearly affected by the installed wind turbines both in the Baltic Sea and in Kattegat, accounting for a maximum reduction of H_{m0} of approximately 0.1 m. Along the coast of Jutland the maximum decrease in wave height is less than 0.05 m.

Results are shown in Figure 7.5 and repeated in Figure 7.6 with marking of windfarm sites.

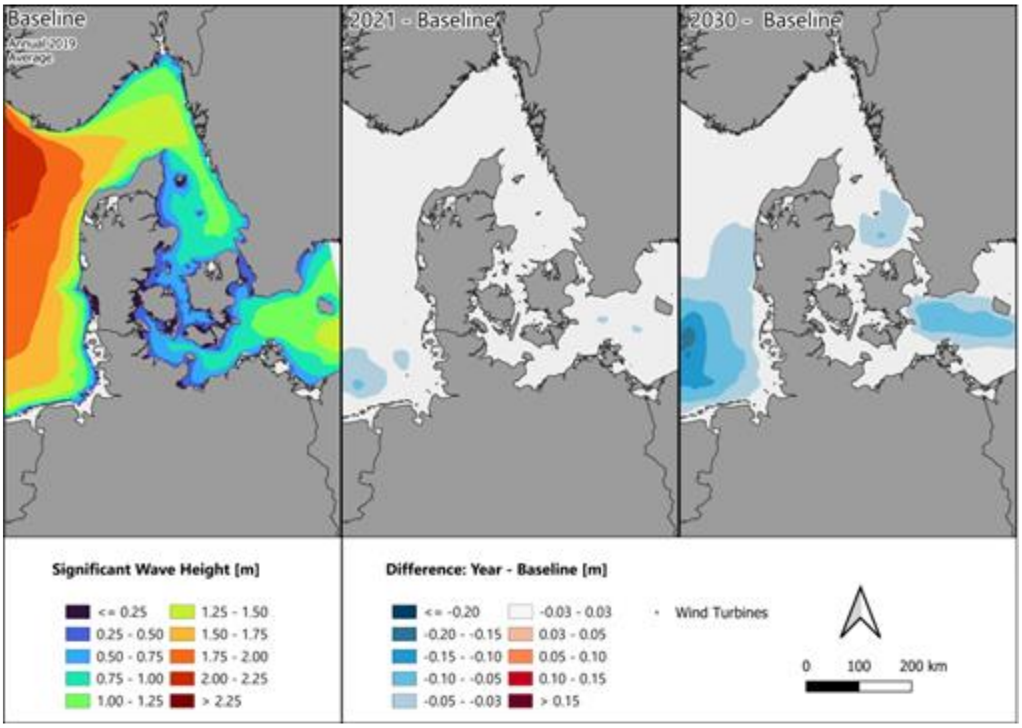

Figure 7.5: ***Danish Waters - Baseline and Baseline - Scenarios.*** *Left: annual average* H_{m0} *(m), Mid: Scenario 2021 minus Baseline, Right: Scenario 2030 minus Baseline.*

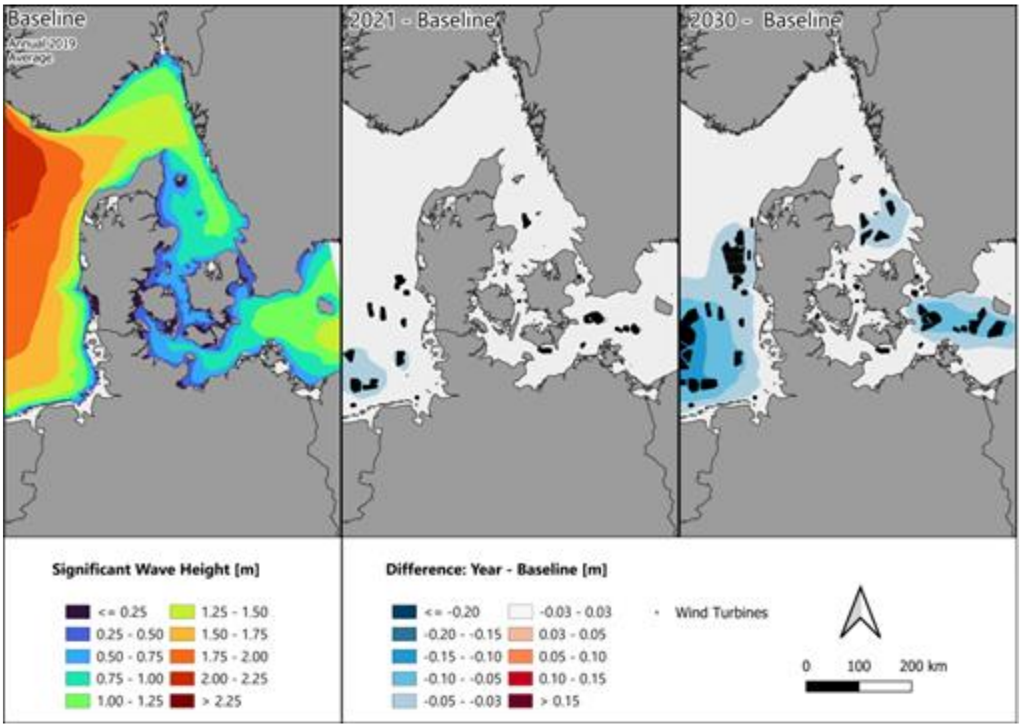

Figure 7.6: ***Danish Waters - Baseline and Baseline - Scenarios.*** *Left: annual* H_{m0} *(m), Mid: Scenario 2021 minus Baseline, Right: Scenario 2030 minus Baseline. "Mid" and "Right" marked with the wind farms.*

Key results for observed seasonal spatial impact:

- In general, the impact of seasonal variation is more readily identifiable in the Future scenario compared to the Current scenario.
- For the Future scenario it reveals that in some months there are minor areas with increasing significant waves, up to 0.03 m in average in February, April and November.
- The largest reduction in the significant wave height is correlated to the general wave height, e.g. a higher average significant wave height result in a larger reduction, for the Future scenario visible in the area with the highest density of wind turbines.
- In other respects, the trend aligns with the annual impact.

The monthly differences, for the entire modelled area and for the Danish EEZ, can be found in Appendix E and Appendix F

7.3. Impact on Sediment Transport Capacity

The development of wind farms in Danish and adjacent waters leads to modifications in wave conditions. These changes may affect the longshore sediment transport capacity, potentially disrupting the natural progression of the shoreline. This impact is assessed for the Current (2021) and Future (2030) scenarios in the North Sea, Kattegat, and the Baltic Sea. The evaluation is conducted by comparing these developments to the Baseline scenario using the Kamphius 1991 formula (see Section 5.2).

To assess the variations in the sediment transport capacity rate due to changes in wind farms along the Danish shores, 12 locations were chosen. The approximate locations and the shore normal[3] at those points are shown in Figure 7.7 (left) and Figure 7.8 (left).

Wave parameters, H_{m0}, T_p and MWD were extracted at each location from the results of the wave model for the three cases and used to calculate the longshore transport for each scenario: Baseline, Current (2021) and Future (2030) scenario. The assumed median grain size is 0.2 mm for all the locations while the bed slope is location specific.

The estimated changes in the longshore transport rates should not be considered representative of actual conditions due to several factors:

- The approximations in the theoretical formulation, such as the disregard for shoreline orientation and cross shore profile variations along the coastline,
- And the lack of data on grain size distribution in the areas analysed.

The estimated sediment transport capacity was exclusively used to evaluate the potential impact of the wind farms on longshore sediment transport capacity, by examining the percentage increases or decreases in either direction relative to the Baseline scenario.

Table 7.2, Figure 7.7 and Figure 7.8 show the impact in sediment transport capacity (%) in both positive and negative directions for each wind farm case (Current and Future scenario) utilizing the year 2019 with respect to the Baseline scenario for the same year. For instance, a positive value signifies an enhancement in sediment transport capacity, whereas a negative value denotes a reduction attributed to the presence of wind farms.

[3] Direction perpendicular to the shoreline.

It is important to clarify that the modifications do not necessarily indicate whether the chosen coastlines will undergo erosion or deposition; rather, they merely denote that a change may occurred.

Key results regarding sediment transport capacity

- As expected, based on the observations regarding the impact on waves, the largest variations in the sediment transport capacity occur for the Future Scenario (2030) – the scenario with the largest spatial reduction in the significant waves,
- The variations in the positive and negative directions mostly follow the same trend for both wind farm scenarios,
- The presence of wind farms mainly generates a decrease in sediment transport capacity in both directions, due to reduction of the significant wave height, but there are locations where the sediment transport potential increases in one direction as a result of changing wave conditions (wave direction),
- The most significant relative changes are noted on the eastern side of Denmark, where the planned development of wind farms will occupy a substantial area compared to the currently available space in the Baltic Sea.

Table 7.2: Indicative changes to the longshore sediment transport for Current and Future scenario. Red (-) reduction and Blue (+) increase in the transport. "Left and "Right" is the sediment transport direction seen for an observer facing the sea.

Case	Sed. trans-port dir.	Jutland west coast					Jutland east coast		Zealand	Køge Bugt	Faxe Buge	Hjelm Bugt	Anholt
		Rømø	Henne Strand	Ferring Strand	Svinkløv	Kandestederne	Gerø Enge	Fornæs	Tisvilde	Mosede	Faxe Ladeplads	Hjelm	Pakhusbugt
		1	2	3	4	5	6	7	8	9	10	11	12
Current - Baseline	"Left"	-1.30 %	+0.61 %	+0.19 %	-0.37 %	-0.90 %	-0.45 %	-1.82 %	-1.20 %	+0.51 %	+1.23 %	-0.69 %	-0.57 %
	"Right"	-0.27 %	-1.90 %	+0.06 %	+0.18 %	+0.43 %	-0.10 %	-0.70 %	+0.67 %	-0.87 %	-3.09 %	-5.21 %	+0.64 %
Future - Baseline	"Left"	-0.21 %	-1.91 %	-1.07 %	-2.80 %	-1.98 %	-1.54 %	-8.31 %	-4.79 %	-6.92 %	-2.06 %	-3.25 %	-8.11 %
	"Right"	-6.32 %	-4.09 %	-4.02 %	+0.55 %	+1.14 %	+0.20 %	-0.29 %	-0.89 %	-2.96 %	-17.67 %	-18.23 %	-2.23 %

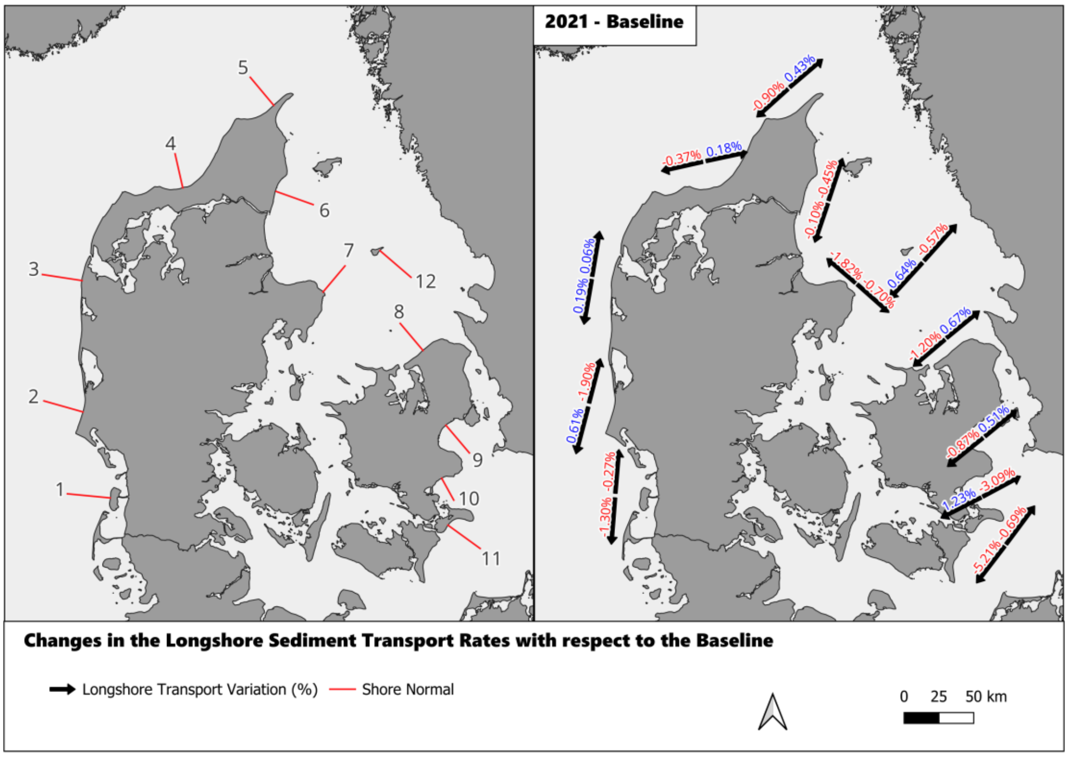

Figure 7.7: Variations (%) in longshore sediment transport capacity for the Current scenario compared to the Baseline: red to indicate a decrease and in blue to indicate an increase.

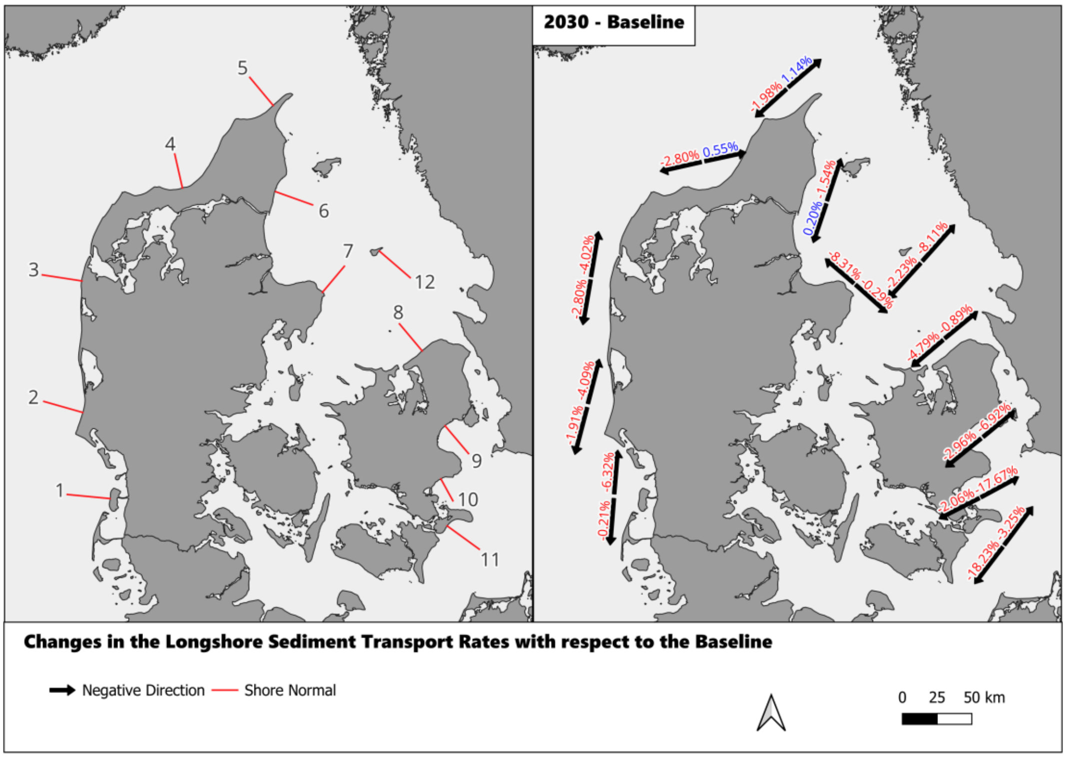

Figure 7.8: Variations (%) in longshore sediment transport capacity for the Future scenario compared to the Baseline scenario: red to indicate a decrease and in blue to indicate an increase.

8. Discussion

The results reveal identifiable trends in how different offshore wind farm configurations affect wave climate and sediment transport capacity. Simulations show a noticeable reduction in significant wave height (H_{m0}) and a corresponding decline in sediment transport capacity under both the Current and the Future scenario compared to the Baseline scenario. However, the significance of these changes, such as a 0.2 m drop in H_{m0} or an 18% reduction in sediment transport capacity, requires further context to determine their practical impact.

It is crucial to note that the reductions in Hm0 are presented as annual averages. Consequently, under specific conditions such as storm events or periods of elevated wave energy, the effects could be more pronounced (potentially exceeding a reduction of 0.2 meters). This could lead to a more significant decrease in wave energy within the system, thereby exerting a stronger influence on sediment dynamics.

Based on the results presented in Table 7.2, Figure 7.7 and Figure 7.8, the areas most impacted by changes in wave conditions, and consequently showing the greatest increase or decrease in sediment transport capacity, are Faxe Bugt and Hjelm Bugt, corresponding to locations 10 and 11, respectively.

In fact, Figure 7.3 and Figure 7.5 clearly show that the shorelines influenced by the wind farms in the Baltic Sea is likely linked to the fetch with a density of wind turbines in Danish, Swedish and German waters as the majority of wave energy in this area reaches the coast og Falster, Møn and Zealand correspond to the direction with the longest fetch.

Although the findings indicate that offshore wind farms may affect coastal processes, the current analysis utilizing longshore transport capacity does not yield sufficient data to draw definitive conclusions about long-term shoreline evolution or morphological changes associated with actual longshore sediment transport.

As mentioned, the sediment transport capacity is the theoretical upper limit of sediment that waves and currents can carry under specific hydrodynamic conditions. It reflects the potential for sediment movement, based on the assumption that sediment is abundantly available. On the other hand, actual sediment transport is the real amount of sediment that is actually moved by the flow at a specific time and place. This depends not only on the transport capacity but also on sediment availability, grain size, bed composition, and other environmental factors like vegetation or human-made structures.

This distinction is crucial as it highlights why, even though the Kamphuis formulation accounts for grain size and bed slope, additional research is necessary to capture local variability, pinpoint the most vulnerable areas, and validate the results with observational data. In fact, more comprehensive sediment budgets, long-term morphological modelling, and sensitivity analyses would provide a stronger foundation for more accurate conclusions.

9. References

DHI A/S. 2021. *MIKE 21 Spectral Wave Module. Scientific Documentation.* Hørsholm : s.n., 2021.

EMODnet. 2023. Bathymetry. *portal.emodnet-bathymetry.eu/#.* [Online] 15 03 2023. portal.emodnet-bathymetry.eu/#.

German Federal Maritime and Hydrographic Agency (BSH). 2021. *Report on the oceanographic conditions at site O-1.3.* 2021.

Hahmann, Andrea N., et al. 2025. *Environmental Mapping and Screening of the Offshore Wind Potential in Denmark, Sensitivity mapping: Wind.* s.l. : DTU Department of Wind and Energy Systems, 2025.

Howard, Katherine, et al. 2009. THE IMPACT OF ATMOSPHERIC MODEL RESOLUTION ON A COUPLED WIND/WAVE FORECAST SYSTEM. 2009.

Leo Vanrjin, Delft, Netherlands. LONGSHORE SAND TRANSPORT. [Online] https://www.leovanrijn-sediment.com/papers/P3-2002a.pdf.

Ute Daewel, Naveed Akhtar, Nils Christiansen & Corinna Schrum. 2022. Offshore wind farms are projected to impact primary production and bottom water deoxygenation in the North Sea. *communications earth & environment.* 2022.